

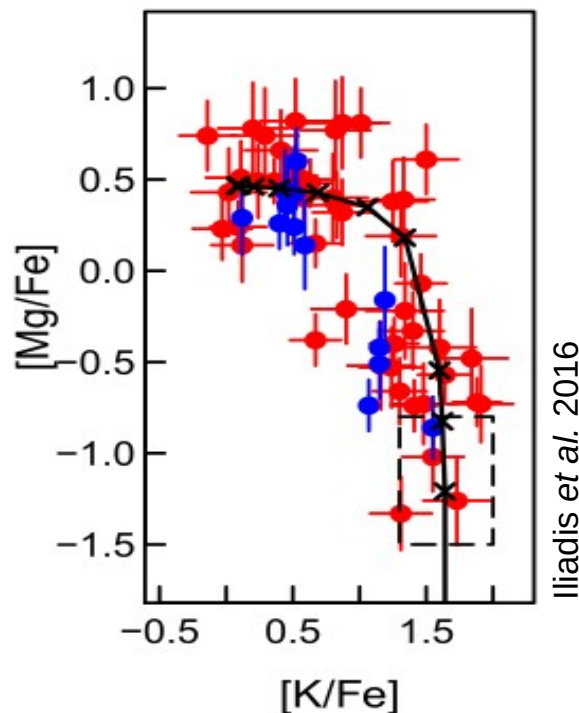
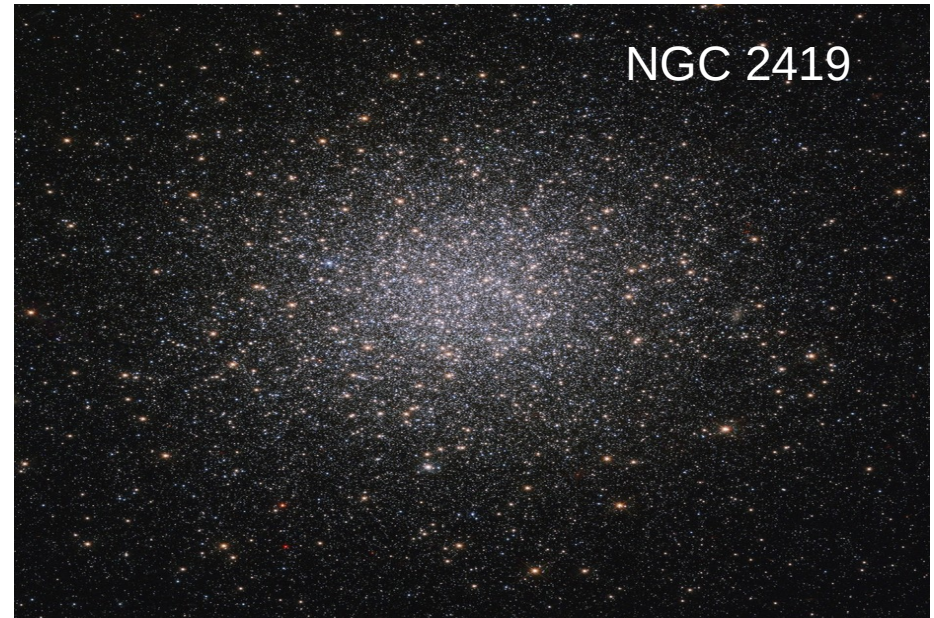
# Understanding elemental anomalies in Globular Clusters: Experimental study of the $^{30}\text{Si}(p,\gamma)^{31}\text{P}$ reaction

Djamila Sarah HARROUZ

Supervisors:  
Nicolas de Séréville  
Faïrouz Hammache

# Globular Clusters

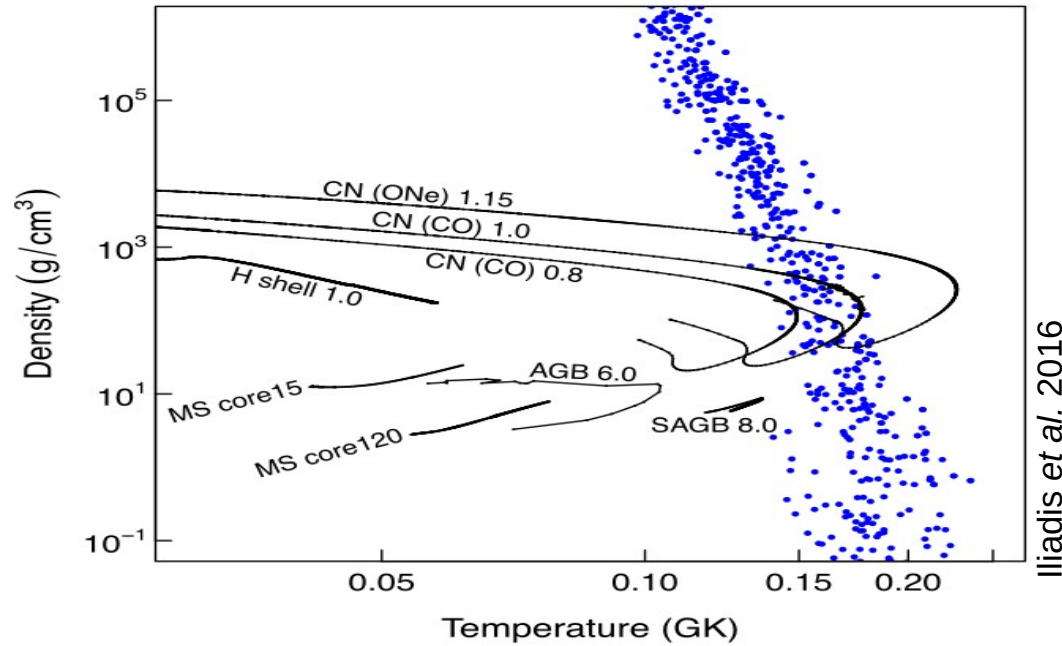
- Dense collection of stars ( $10^5$ - $10^7$ ) orbiting around the center of the Galaxy.
- Independent probes of the age and early chemical history of the Universe.
- Privileged sites for understanding stellar formation. Paradigm: unique stellar population (generation)



**Observation :** anticorrelation between pairs of chemical species, inconsistent with the current temperature of the stars  
→ Shift in the paradigm: Globular clusters may have hosted **different generations of stars**.

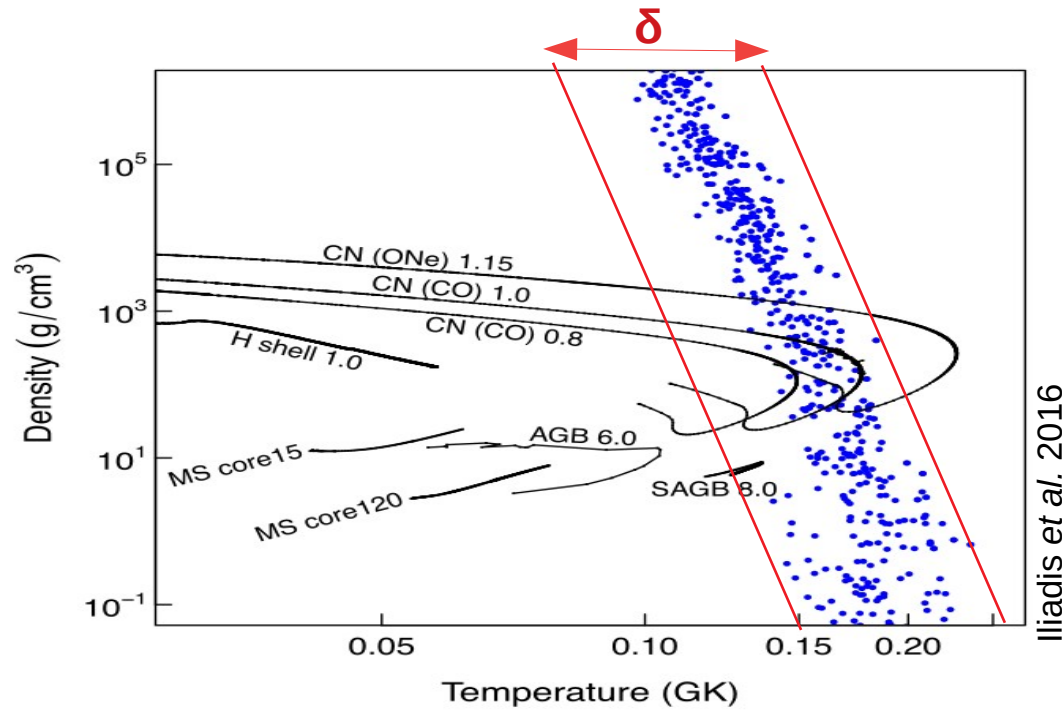
**What are the types of stars that were the site of nuclear reactions that engendered these anticorrelations → Polluter candidates ?**

# Reactions of interest



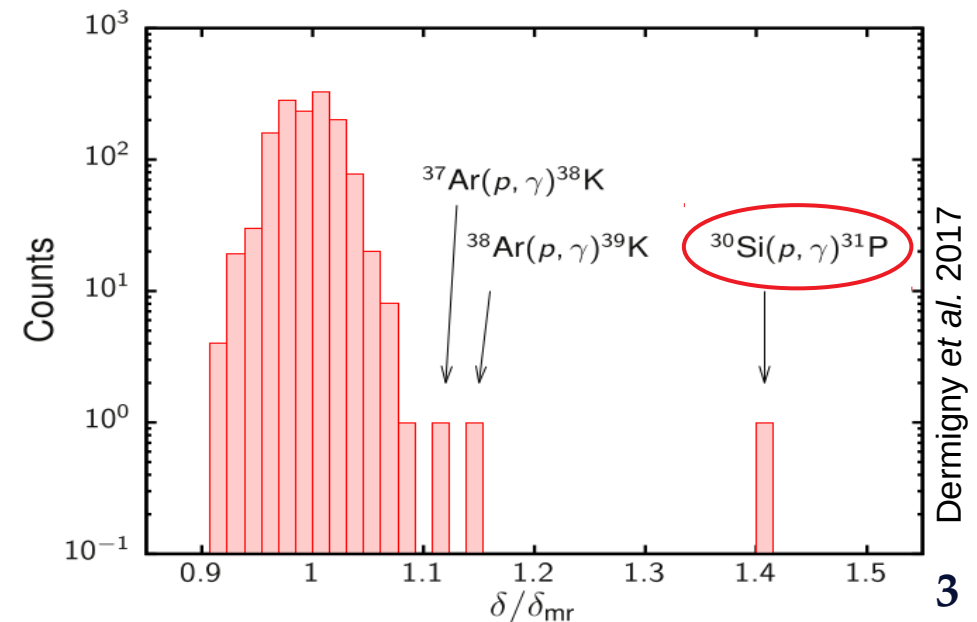
- Each  $(T, \rho)$  point reproduces the observed abundances in Globular Clusters.
- The abundances are estimated by simulating a network of nuclear reactions occurring at a given  $(T, \rho)$  set.
- Conditions corresponding to Hydrogen burning stage.

# Reactions of interest



- Impact of the reactions and their uncertainty is identified with a Monte Carlo sensitivity study.
- Si reaction contributes the most to the spread of the  $(T, \rho)$  locus.

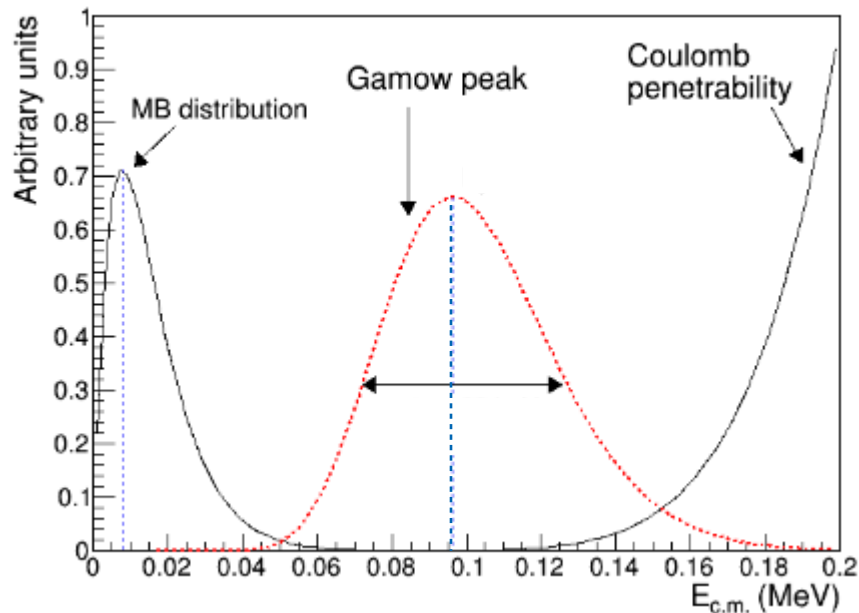
- Each  $(T, \rho)$  point reproduces the observed abundances in Globular Clusters.
- The abundances are estimated by simulating a network of nuclear reactions occurring at a given  $(T, \rho)$  set.
- Conditions corresponding to Hydrogen burning stage.



# Thermonuclear reaction rate

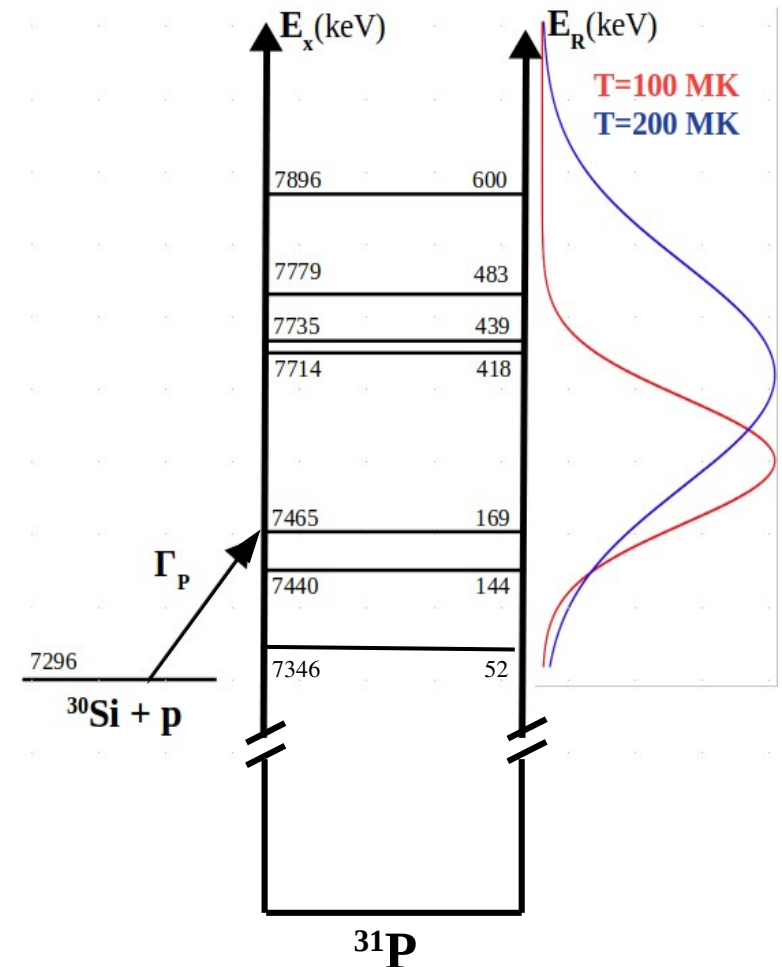
The thermonuclear reaction rate is defined as :

$$\langle \sigma v \rangle = \left( \frac{8}{\pi \mu} \right)^{1/2} \frac{1}{(kT)^{3/2}} \int_0^{\infty} E \sigma(E) e^{-E/kT} dE$$



Narrow resonances  $\langle \sigma v \rangle \propto \sum_i \omega \gamma_i e^{\frac{-E_{Ri}}{kT}}$

Resonance strength  $\omega \gamma = \frac{2J_R + 1}{(2J_p + 1)(2J_{^{30}\text{Si}} + 1)} \frac{\Gamma_p \Gamma_\gamma}{\Gamma}$



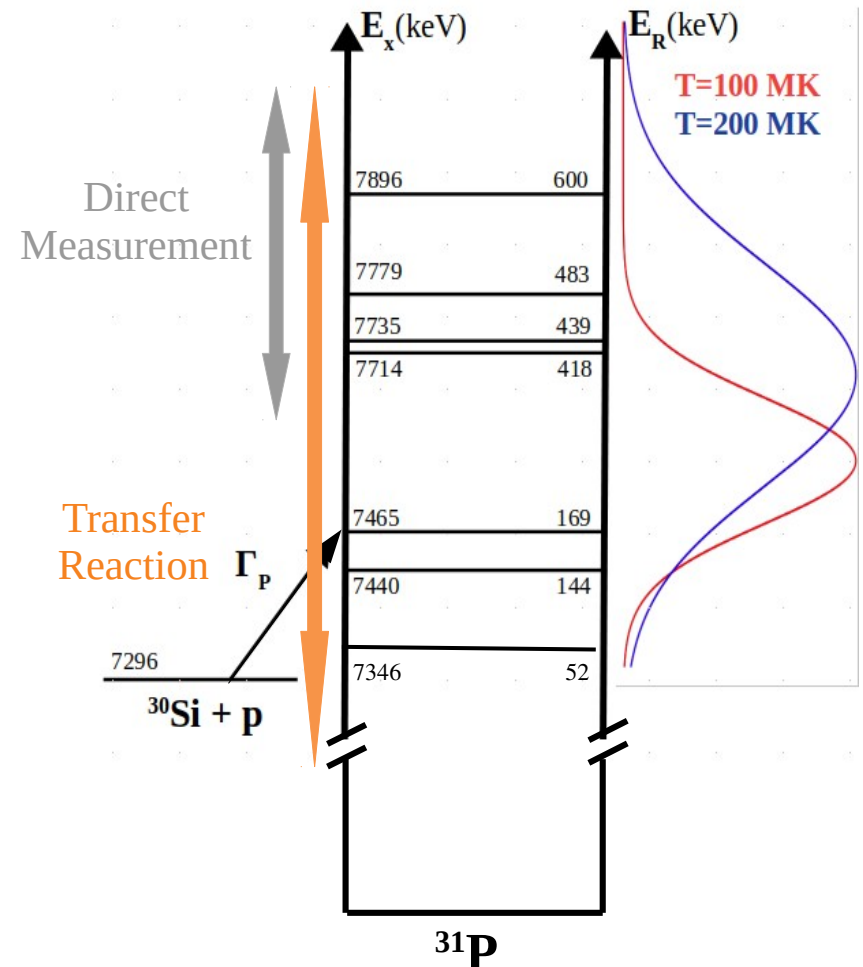
In our case  $\begin{cases} \Gamma = \Gamma_p + \Gamma_\gamma \\ \Gamma_p \ll \Gamma_\gamma \end{cases} \Rightarrow \omega \gamma \propto \Gamma_p$

# State of the art for $^{30}\text{Si}(p,\gamma)^{31}\text{P}$ reaction

Several measurements performed for  $E_r > 600$  keV  
Last one published by **Dermigny *et al.* 2020**,  
resonance strengths measured through gamma  
spectroscopy.

Experiment performed by **J.Vernotte in 1990** at  
Orsay's SplitPole:  $^{30}\text{Si}(^3\text{He},d)^{31}\text{P}$

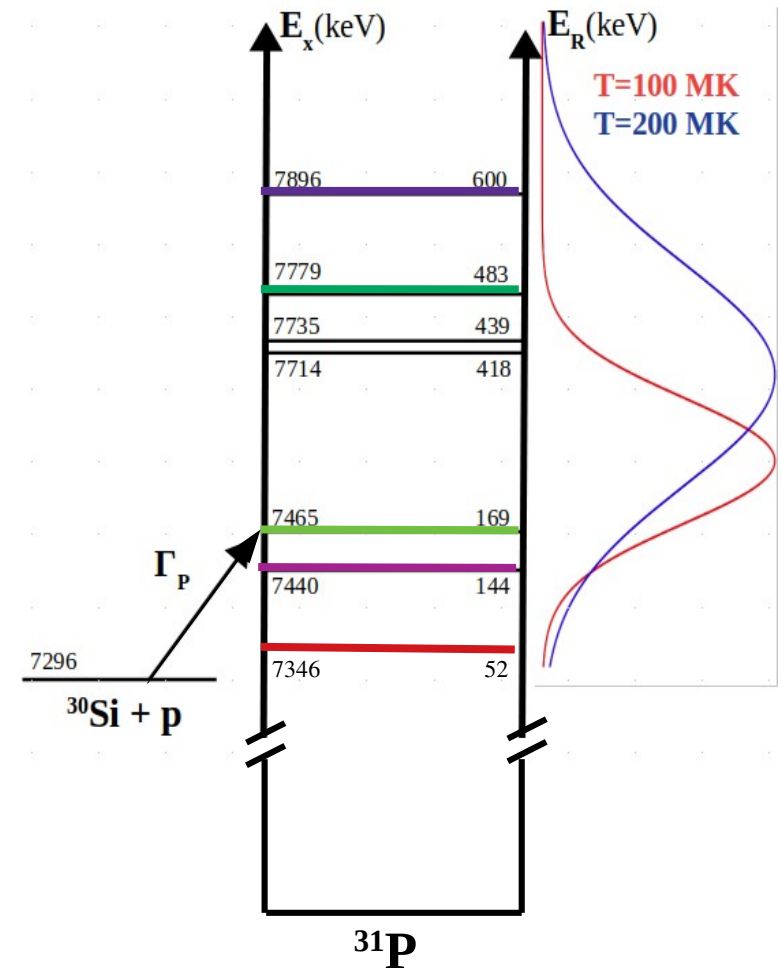
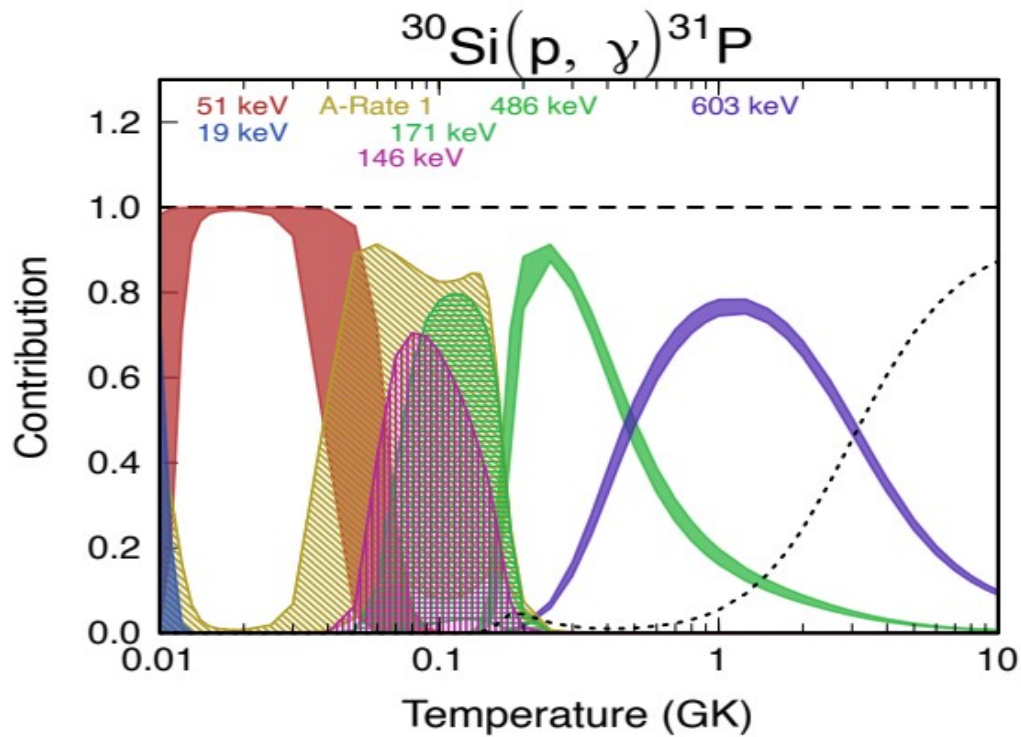
- No astrophysical motivations: did not observe the states at 7.440 and 7.465 MeV.
- The resolution did not allow the separation of the 7.714 - 7.735 MeV doublet.





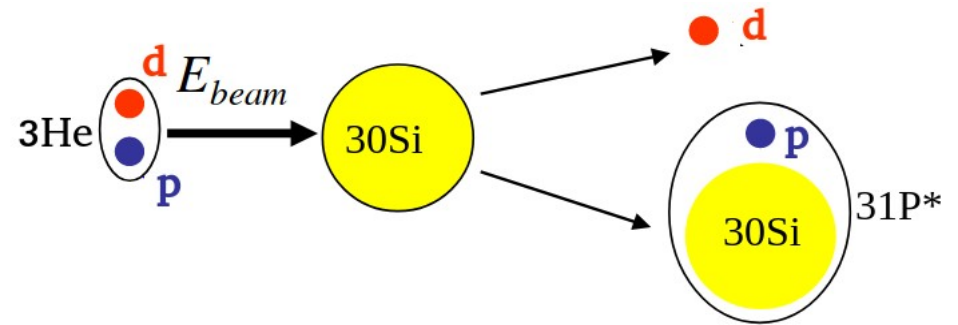
# State of the art for $^{30}\text{Si}(p,\gamma)^{31}\text{P}$ reaction

Dermigny et al. 2020



# Transfer Reaction

Compare the experimental angular distribution to the one obtained from a model describing the direct transfer process:





# Transfer Reaction

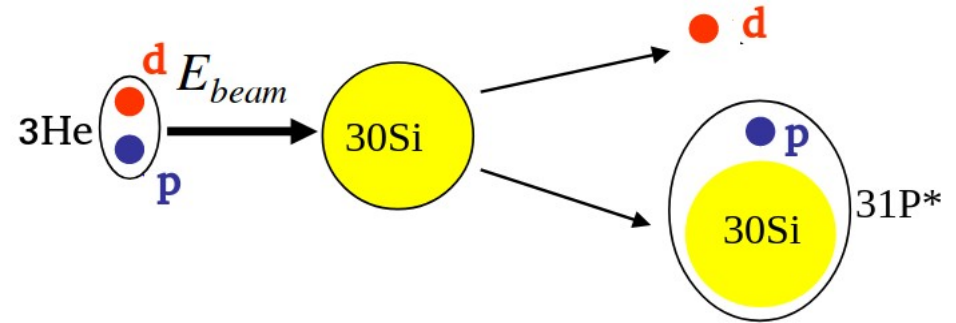
Compare the experimental angular distribution to the one obtained from a model describing the direct transfer process:

- Normalisation:

$$\frac{d\sigma}{d\Omega}(\theta)_{\text{exp}} = C^2 S_{lj} \frac{d\sigma}{d\Omega}(\theta)_{\text{DWBA}}$$

$$\Gamma_p = C^2 S_{lj} \Gamma_p^{\text{single particle}}(E_r, l)$$

- Shape of the distribution → transferred angular orbital momentum  $l$



# Transfer Reaction

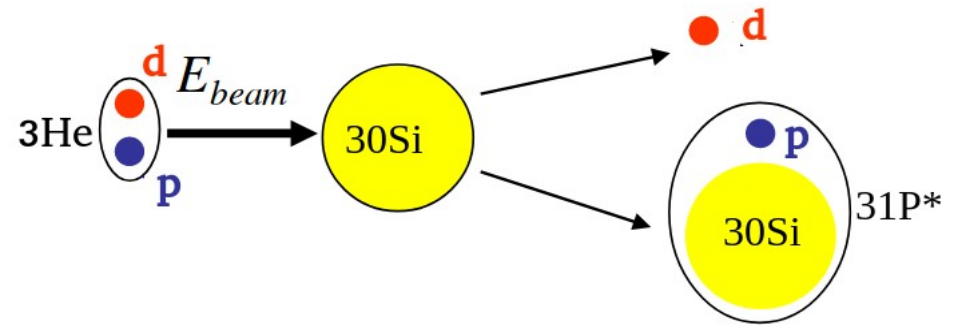
Compare the experimental angular distribution to the one obtained from a model describing the direct transfer process:

- Normalisation:

$$\frac{d\sigma}{d\Omega}(\theta)_{\text{exp}} = C^2 S_{lj} \frac{d\sigma}{d\Omega}(\theta)_{\text{DWBA}}$$

$$\Gamma_p = C^2 S_{lj} \Gamma_p^{\text{single particle}}(E_r, l)$$

- Shape of the distribution → transferred angular orbital momentum  $l$

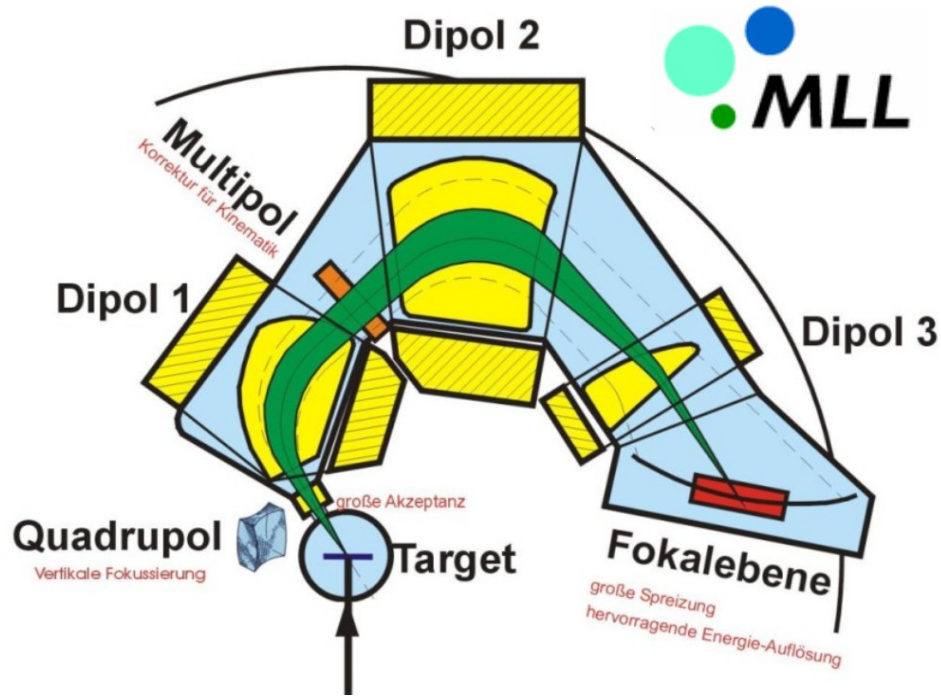


*Distorted Wave Born Approximation* :

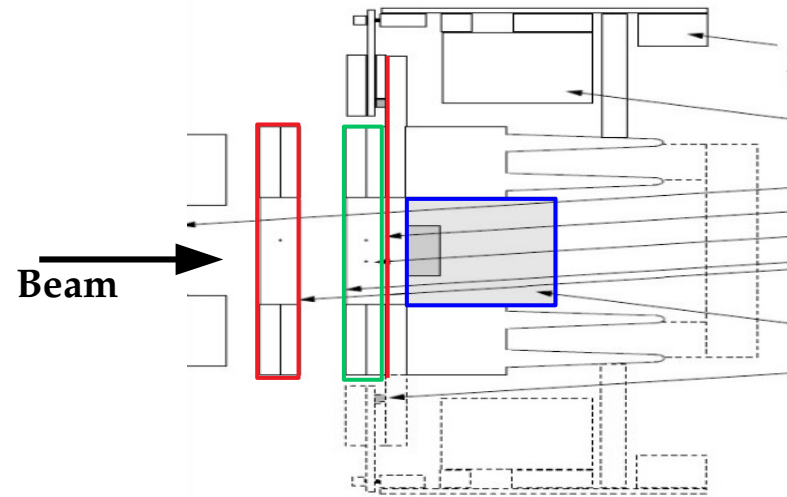
- Entrance and exit channels are dominated by elastic scattering.
- The transfer of the nucleon is a first order perturbation.
- No configuration rearrangement in the composite nucleus.

**Main ingredients:** optical potentials describing elastic channels.

# Q3D experiment



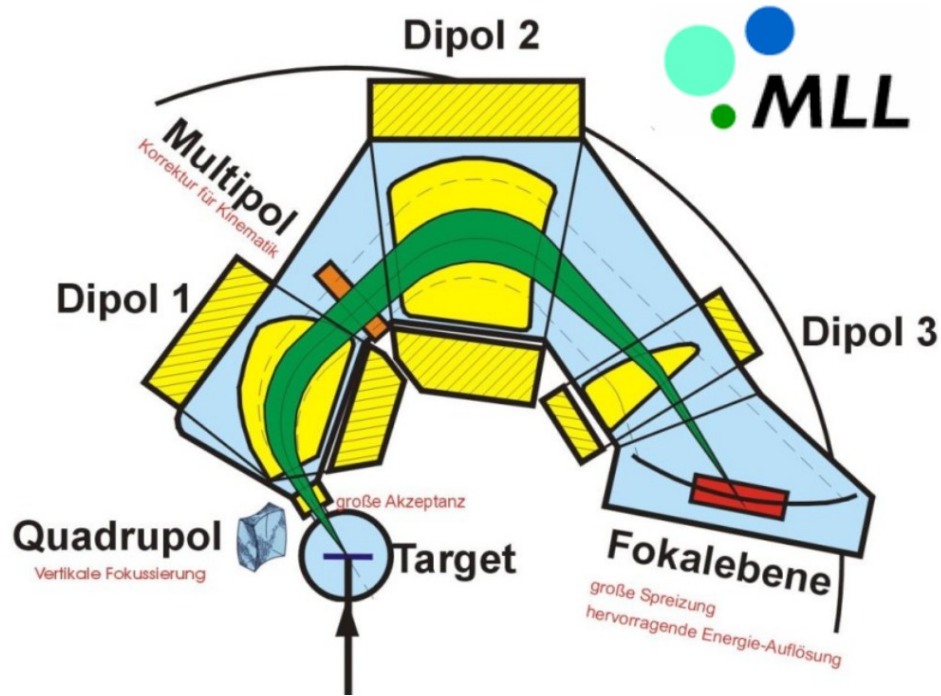
- Beam  $^3\text{He}$  :  $E = 25 \text{ MeV}$   
 $I = 200 \text{ nAe}$
- Targets:  $^{30}\text{SiO}_2$  ( $40 \mu\text{g}/\text{cm}^2$ ) enriched at 95% on  $^{\text{nat}}\text{C}$   
 $^{\text{nat}}\text{SiO}_2$  ( $20 \mu\text{g}/\text{cm}^2$ ) on  $^{\text{nat}}\text{C}$
- Solid Angle :  $4 - 12 \text{ msr}$
- Energy resolution  $\Delta E/E \sim 2.10^{-4}$



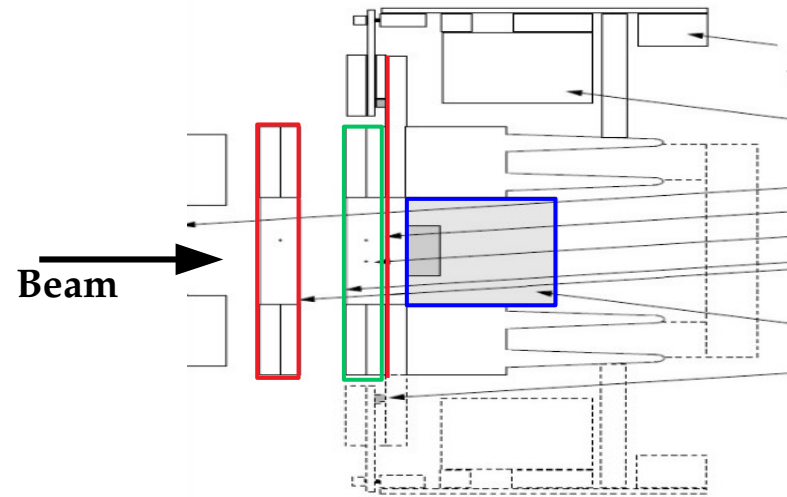
Focal plan detectors :

- **Gaz detector & strips** → position on the focal plane.
- **Ionisation chamber** → energy loss.
- **Plastic scintillator** → residual energy.

# Q3D experiment

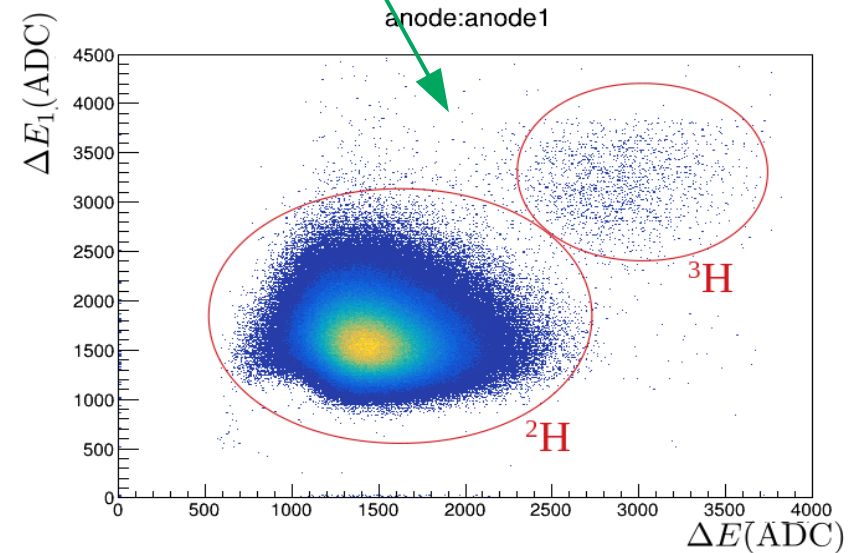


- Beam  $^3\text{He}$  :  $E = 25 \text{ MeV}$   
 $I = 200 \text{ nAe}$
- Targets:  $^{30}\text{SiO}_2$  ( $40 \mu\text{g}/\text{cm}^2$ ) enriched at 95% on  $^{\text{nat}}\text{C}$   
 $^{\text{nat}}\text{SiO}_2$  ( $20 \mu\text{g}/\text{cm}^2$ ) on  $^{\text{nat}}\text{C}$
- Solid Angle :  $4 - 12 \text{ msr}$
- Energy resolution  $\Delta E/E \sim 2 \cdot 10^{-4}$



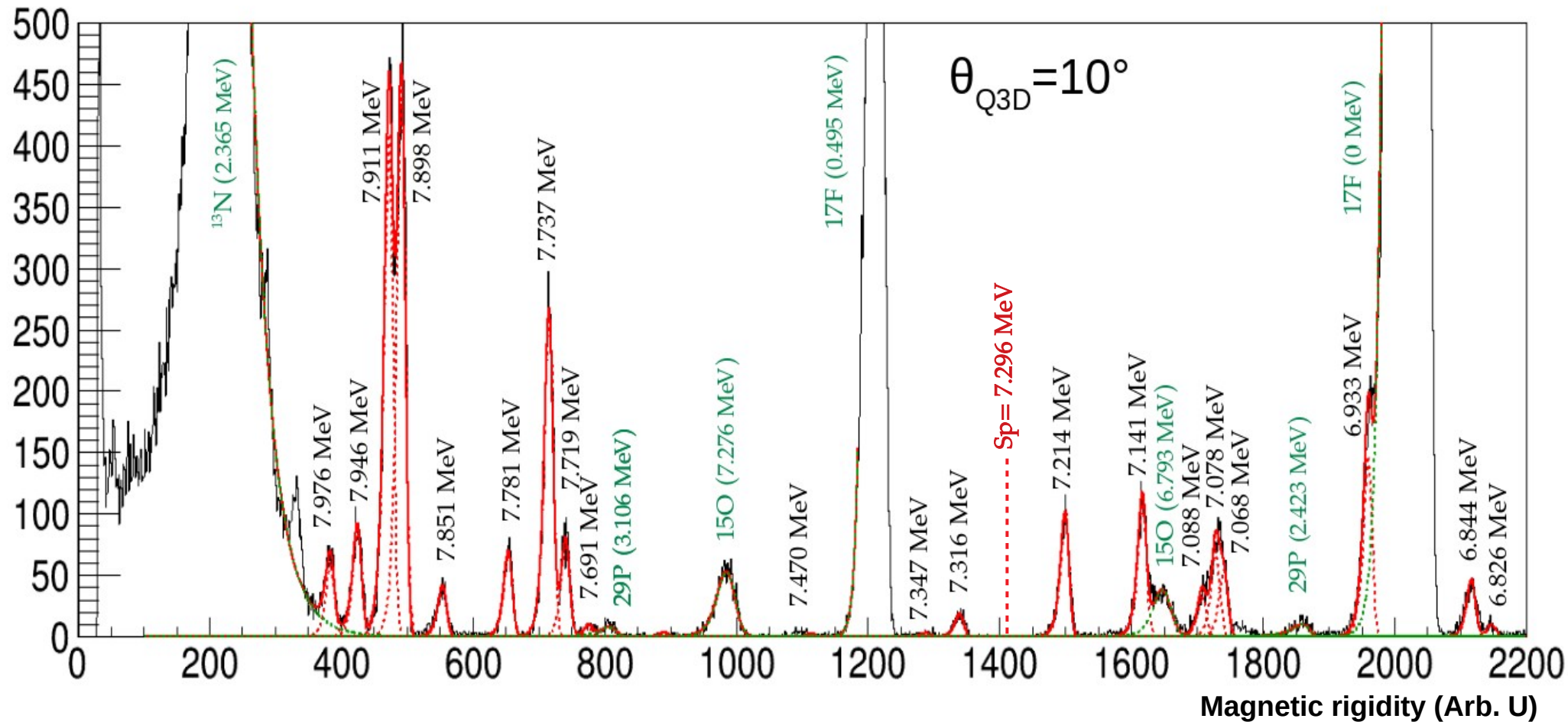
Focal plan detectors :

- **Gaz detector & strips** → position on the focal plane.
- **Ionisation chamber** → energy loss.
- **Plastic scintillator** → residual energy.



# Spectrum

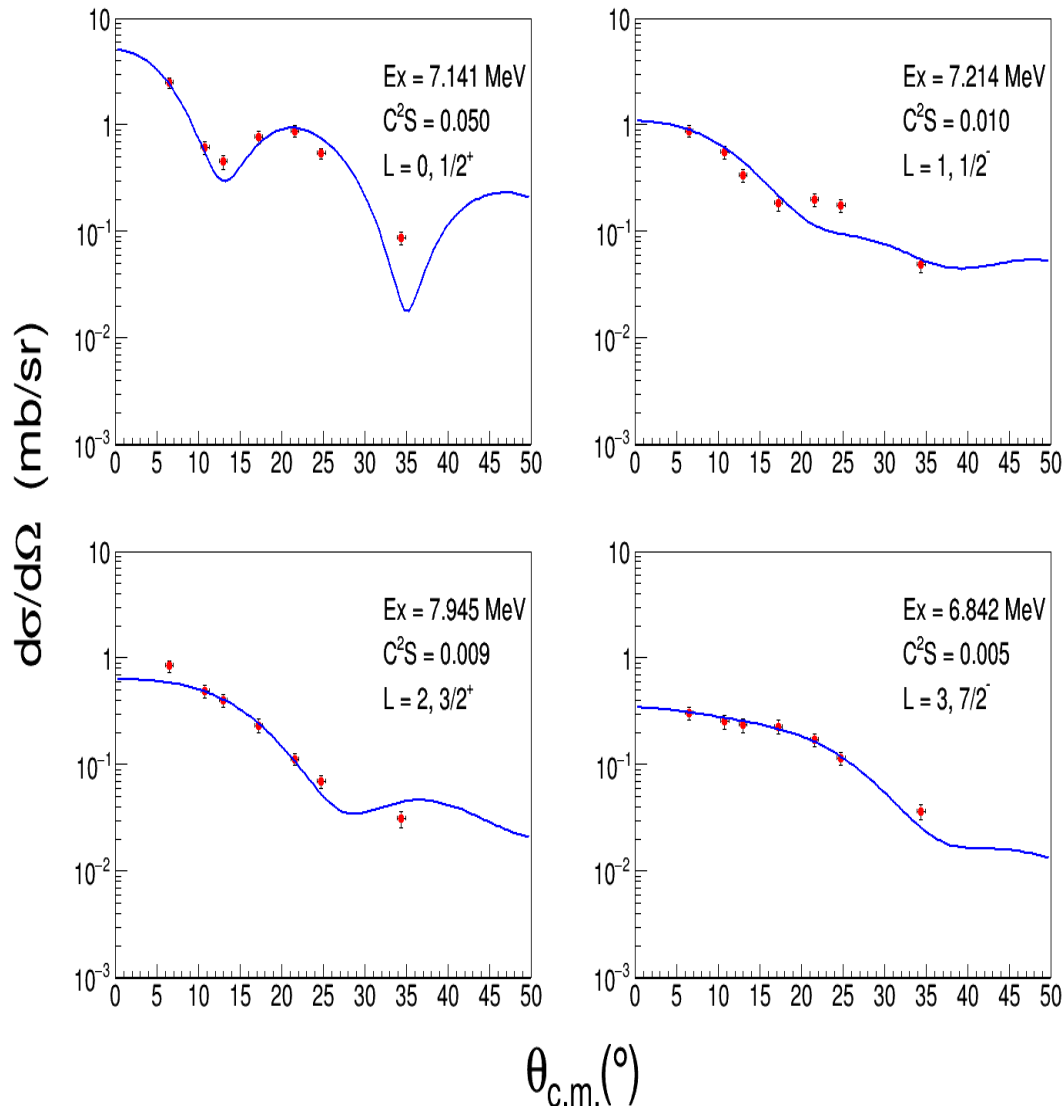
Counts



- Spectra for 7 lab angles :  $6^\circ$ ,  $10^\circ$ ,  $12^\circ$ ,  $16^\circ$ ,  $20^\circ$ ,  $23^\circ$ ,  $32^\circ$
- Experimental resolution FWHM  $\sim 7 \text{ keV}$   
Vernotte (1990)  $\sim 25 \text{ keV}$

- **Doublet at 7719 - 7737 keV separated**
- **Level at 7470 keV observed.**
- **Indications about the 7440 keV level.**

# Angular distributions



Differential cross section

$$\frac{d\sigma}{d\Omega}(\theta)_{\text{exp}} = \frac{N_{\text{counts}}}{N_{\text{beam}} \cdot N_{\text{target}} \cdot \Delta\Omega} = C^2 S_{lj} \frac{d\sigma}{d\Omega}(\theta)_{\text{DWBA}}$$

Finite-Range DWBA calculations performed with **FRESCO code**.

Once the spectroscopic factor is estimated from the transfer reaction, we can compute:

- the proton width:  $\Gamma_p = C^2 S_{lj} \Gamma_p^{\text{single particle}}(E_r, l)$

- the resonances strengths:

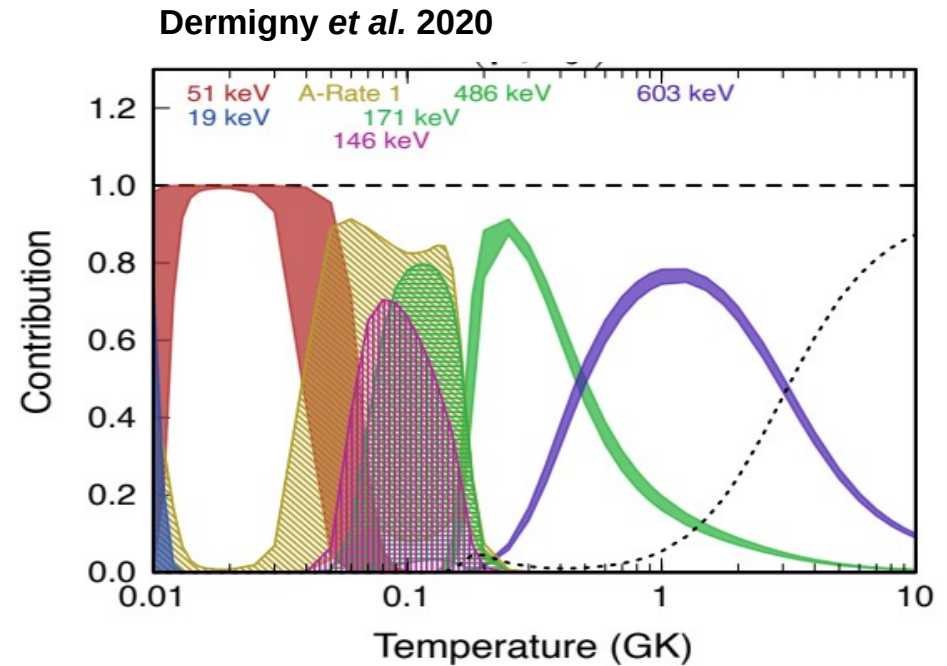
$$\omega \gamma = \frac{2J_R + 1}{(2J_p + 1)(2J_{30\text{Si}} + 1)} \Gamma_p$$

- Uncertainties  $\sim 30\%$  (optical potentials)



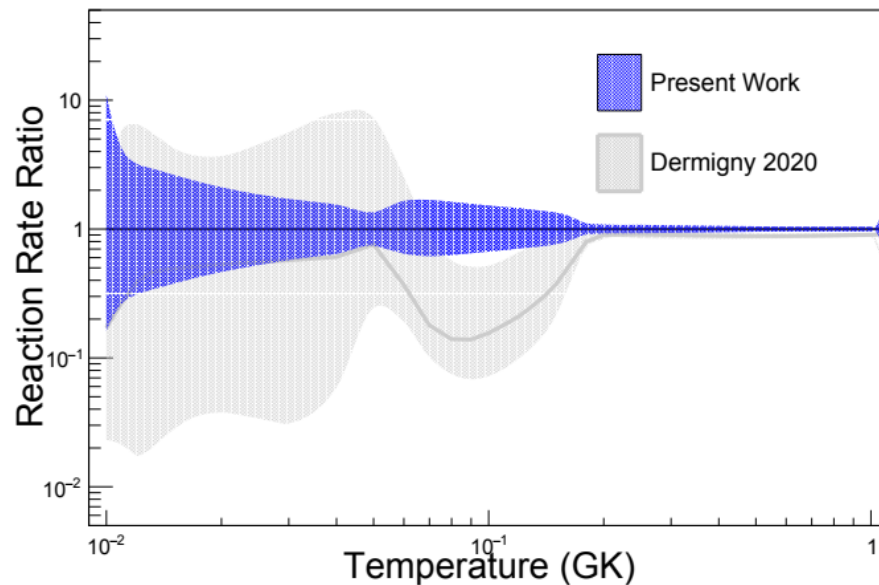
# Results

- Doublet separation → strong constraints on the spin of low component ( $E_r = 418$  keV,  $l=3$ ).
- Good agreement for strength values (within 50%) with direct measurements ( $E_r = 486$  keV)

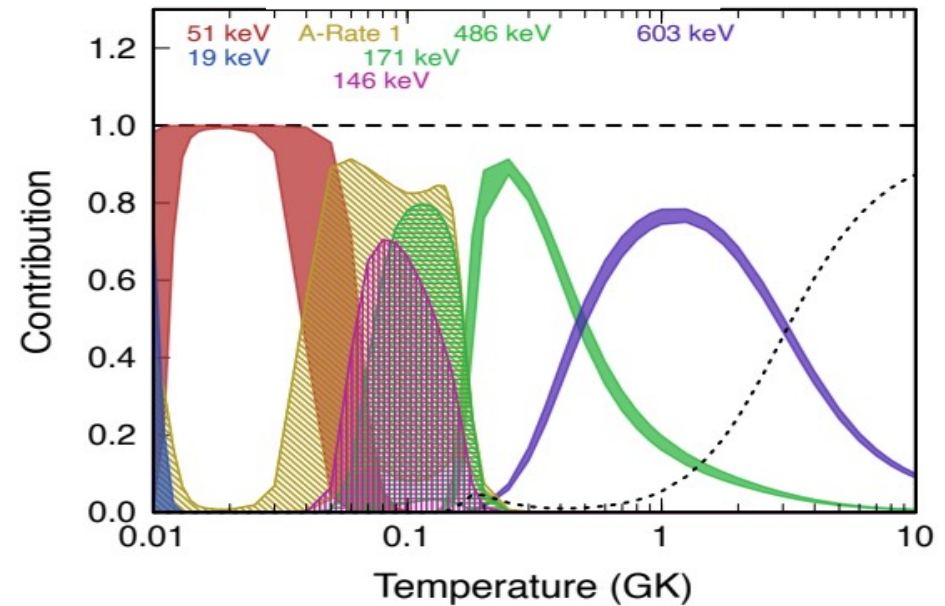


# Results

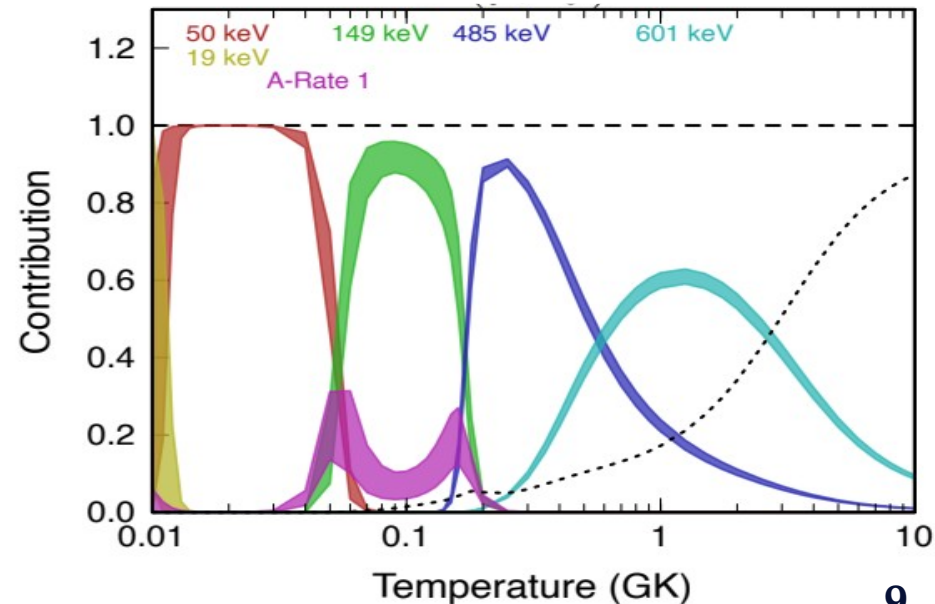
- Doublet separation → strong constraints on the spin of low component ( $E_r = 418$  keV,  $l=3$ ).
- Good agreement for strength values (within 50%) with direct measurements ( $E_r = 485$  keV)
- Positive measurement of low energy resonances that were considered upper limits previously ( $E_r = 19$  keV,  $E_r = 51$  keV and  $E_r = 170$  keV)
- Observation of the  $E_r = 149$  keV which is a key resonance in the temperature range of interest (spin have to be better constrained).



Dermigny *et al.* 2020



Harrouz *et al.* (2021) in Prep.



# Conclusions

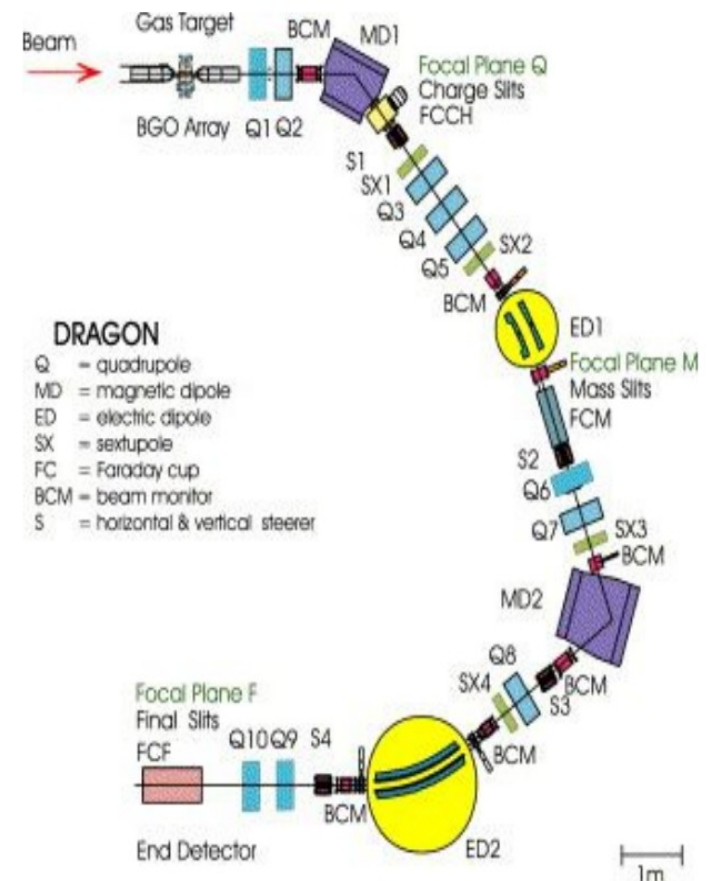
- Extraction of spectroscopic information for the  $^{31}\text{P}$  nucleus between  $E_x = 6800 - 8100$  keV.
- Calculation of strengths for resonances up to  $E_r = 600$  keV.
- Improved determination of the  $^{30}\text{Si}(p,\gamma)^{31}\text{P}$  reaction rate.

# Conclusions

- Extraction of spectroscopic information for the  $^{31}\text{P}$  nucleus between  $E_x = 6800 - 8100$  keV.
- Calculation of strengths for resonances up to  $E_r = 600$  keV.
- Improved determination of the  $^{30}\text{Si}(p,\gamma)^{31}\text{P}$  reaction rate.

## Perspectives

- Perform direct measurement of  $^{30}\text{Si}(p,\gamma)^{31}\text{P}$  reaction rate with the Recoil spectrometer DRAGON (experiment rescheduled next August)
- Participation in the analysis of  $^{39}\text{K}(p,\gamma)^{40}\text{Ca}$  reaction for the same research program concerning Globular Clusters.
- Impact of the new measurements on the temperature locus for constraining “the polluter” candidates.



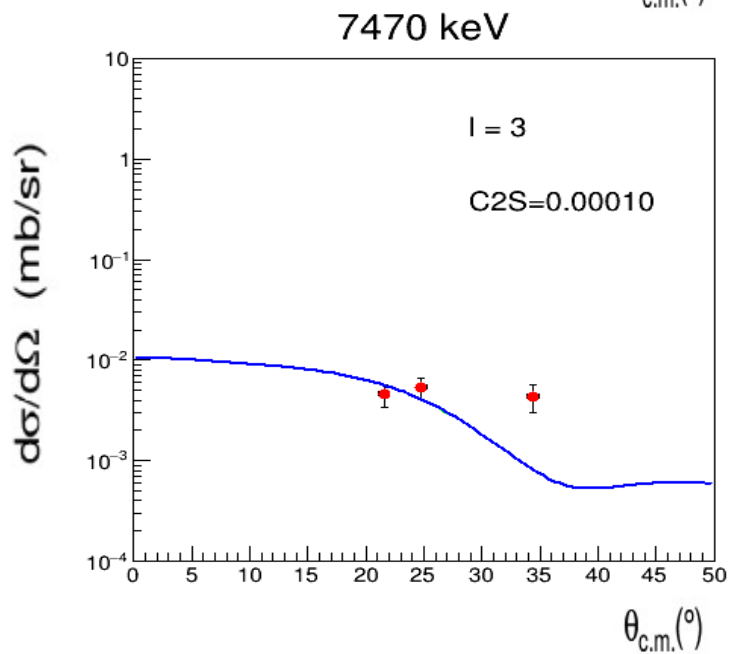
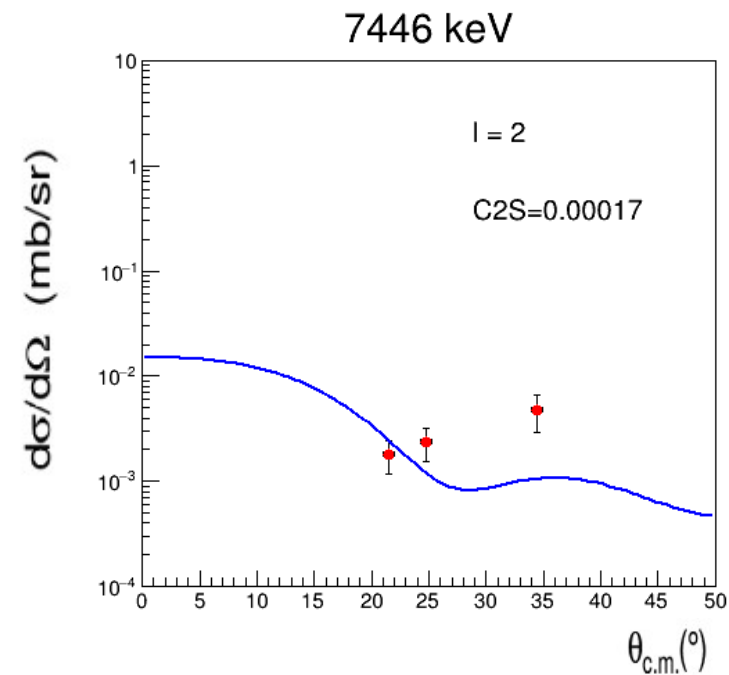
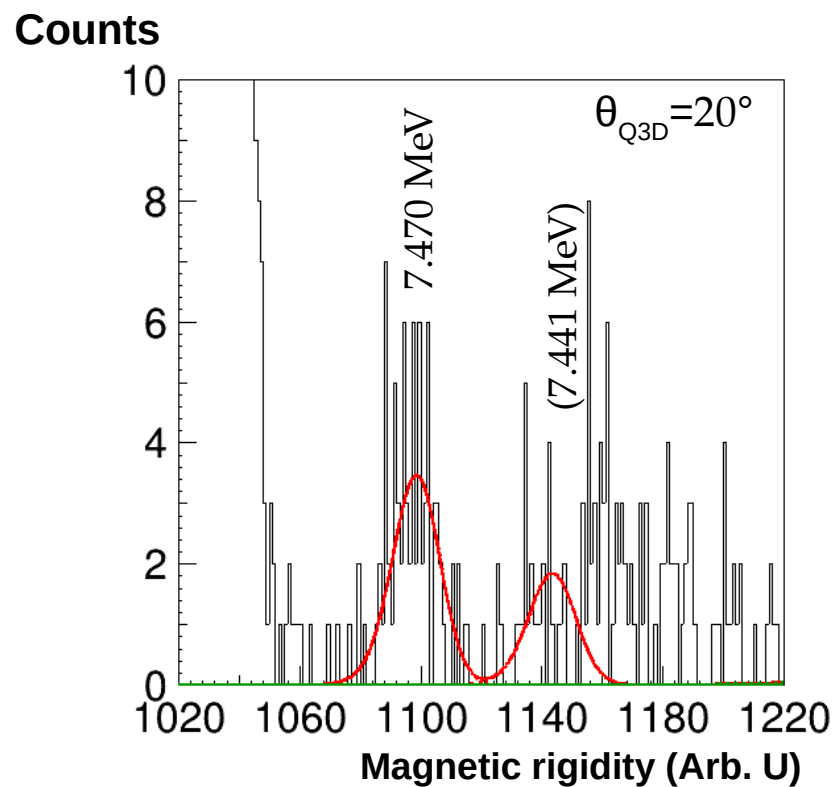
# Thank you for your attention

## Collaborators :

Philip Adsley (iThemba)  
Beyhan Bastin (GANIL)  
Thomas Fastermann (TUM)  
Fairouz Hammache (IJCLab)  
Ralf Hertenberger (TUM)  
Marco La Cognata (LNS)  
Livio Lamia (LNS)  
Richard Longlond (aNCSTU / TUNL)  
Anne Meyer (IJCLab)  
Sara Palmerini (LNS)  
Stefano Romano (LNS)  
Nicolas de Séréville (IJCLab)  
Aurora Tumino (LNS)  
Hans-Friedrich Wirth (TUM)

M13

# Back-up





# Back-up

